Published in final edited form as:
J Magn Reson Imaging. 2010 July ; 32(1): 184–190. doi:10.1002/jmri.22209.

In Vivo Vascular Hallmarks of Diffuse Leukoaraiosis

Jinsoo Uh, PhD, **Uma Yezhuvath, PhD**, **Yamei Cheng, MD**, and **Hanzhang Lu, PhD***
Advanced Imaging Research Center, University of Texas Southwestern Medical Center, Dallas, Texas, USA

Abstract

Purpose—To characterize multiple patterns of vascular changes in leukoaraiosis using in vivo magnetic resonance imaging (MRI) techniques.

Materials and Methods—We measured cerebral blood flow (CBF), cerebrovascular reactivity (CVR), and blood–brain-barrier (BBB) leakage in a group of 33 elderly subjects (age: 72.3 ± 6.8 years, 17 males, 16 females). Leukoaraiosis brain regions were identified in each subject using fluid-attenuated inversion-recovery (FLAIR) MRI. Vascular parameters in the leukoaraiosis regions were compared to those in the normal-appearing white matter (NAWM) regions. Vascular changes in leukoaraiosis were also compared to structural damage as assessed by diffusion tensor imaging.

Results—CBF and CVR in leukoaraiosis regions were found to be 39.7 ± 5.2% ($P < 0.001$) and 52.5 ± 11.6% ($P = 0.005$), respectively, of those in NAWM. In subjects who did not have significant leukoaraiosis, CBF and CVR in regions with high risk for leukoaraiosis showed a slight reduction compared to the other white matter regions. Significant BBB leakage was also detected ($P = 0.003$) in leukoaraiosis and the extent of BBB leakage was positively correlated with mean diffusivity. In addition, CVR in NAWM was lower than that in white matter of subjects without significant leukoaraiosis.

Conclusion—Leukoaraiosis was characterized by reduced CBF, CVR, and a leakage in the BBB.

Keywords

leukoaraiosis; vascular changes; cerebral blood flow; cerebrovascular reactivity; blood-brain-barrier

Leukoaraiosis is defined as diffuse white matter lesions that are often visible on computed tomography (CT) or magnetic resonance imaging (MRI) (1). In particular, these regions appear as hyperintense signals on fluid-attenuated inversion-recovery (FLAIR) MRI (2). Unlike white matter lesions associated with known causes such as stroke or brain tumor, the pathogenesis of leukoaraiosis is not well defined. Previous studies report that leukoaraiosis can be associated with various pathologic conditions including vascular dementia (3), Alzheimer's disease (4), hypertension (5–7), small vessel disease (8–10), atherosclerosis (11), and cerebral hemorrhage (12). Another common cause of leukoaraiosis is aging (13,14). A large majority of elderly individuals have a certain degree of leukoaraiosis, which is most pronounced in the periventricular regions (15–19). There is also evidence that the

*Address reprint requests to: H.L., Advanced Imaging Research Center, UT Southwestern Medical Center, 5323 Harry Hines Blvd., Dallas, TX 75390. hanzhang.lu@utsouthwestern.edu.

amount of leukoaraiosis is predictive of cognitive function (20,21). Therefore, it is important to characterize the physiologic mechanisms underlying age-related leukoaraiosis.

A number of studies have suggested a strong contribution of vascular dysfunction in leukoaraiosis associated with ischemic diseases. Pathologic studies of leukoaraiosis tissue have shown that these regions are characterized by arteriosclerosis and the thickening of the vascular wall as well as a narrowing of the vessel lumen (22,23). Others have postulated that leukoaraiosis is caused by the toxicity of serum protein which leaks into the extravascular tissue when the blood–brain-barrier (BBB) is compromised (24–26). In the present study we aimed to assess whether vascular components also play an important role in age-related leukoaraiosis.

The brain vasculature in leukoaraiosis under in vivo conditions has previously been difficult to assess for two possible reasons. First, the perfusion values of white matter are intrinsically lower than that of gray matter (27), thus accurate measurement of white matter perfusion is not trivial. Second, diffuse leukoaraiosis lesions are small and the spatial resolution of the imaging modality needs to be sufficiently high in order to minimize partial volume effects from surrounding normal tissue. Recent advances in high-field MR systems as well as the development of novel MR sequences have allowed the mapping of various physiological parameters in the brain. In the present work we conducted a multiparametric assessment of vascular parameters to gain a better understanding of physiological hallmarks in leukoaraiosis in elderly subjects. Since we are interested in the pathogenesis of diffuse white matter lesions in the absence of clinically defined vascular diseases, we only selected participants who did not have overt cerebral infarction or lacunae.

In this cross-sectional study we first tested whether cerebral blood flow (CBF) in leukoaraiosis regions was reduced compared to normal-appearing white matter (NAWM). Considering that CBF reduction may not be specific to vascular damage, we also measured the vasodilatory capacity of the vessels using CO_2 inhalation. As a control study, we assessed whether such deficits were also present in subjects who did not have significant leukoaraiosis. In another group of subjects, the leakage of the BBB was assessed using an MR contrast agent. We further assessed the correlation between the extent of BBB leakage and tissue structural integrity as measured by diffusion tensor imaging (DTI).

Materials and Methods

Participants

This study enrolled 33 elderly subjects (age: 72.3 ± 6.8 years, 17 males, 16 females) who did not have brain tumor, dementia, history of stroke, or MRI evidence of cerebral infarction or lacunae. Other inclusion/exclusion criteria were: 1) no contraindication to MRI scanning (pacemaker, implanted metallic objects, neurostimulator); 2) general good health with no serious or unstable medical conditions including major neurological or psychiatric disorders; 3) age greater than 50. The Health Insurance Portability and Accountability Act (HIPAA) compliant protocol was approved by the Institutional Review Board and written informed consent was obtained from all subjects.

MRI Methods

The MRI scans were performed on a 3T MR system (Philips Medical Systems, Best, Netherlands) using a body coil for radiofrequency transmission and an 8-channel head coil with parallel imaging capability for signal reception.

Leukoaraiosis was assessed by hyperintense signals in FLAIR MRI. FLAIR images were acquired in the transverse plane with imaging parameters of field of view (FOV) = 230 ×

230 mm^2, acquisition resolution = 0.65 (anterior–posterior) × 0.87 (right–left) mm^2 (*k*-space matrix size = 352 × 264), reconstructed resolution = 0.45 × 0.45 mm^2, number of slices = 24, slice thickness = 5 mm (gap = 1 mm), TI = 2800 msec, TR/TE = 11000 msec/150 msec, echo train length = 27, SENSE factor = 2, and duration = 3.6 minutes.

Three vascular parameters were measured. Baseline CBF and cerebrovascular reactivity were determined in 17 subjects. BBB leakage was assessed in another group of 16 subjects.

Baseline CBF was measured using a pseudo-continuous arterial spin-labeling (PCASL) technique (28–30) with the following parameters: labeling duration = 1632 msec, TI = 1525 msec, labeling offset = −96 mm, TR/TE/flip angle = 3970msec/14msec/90°, SENSE factor = 2.5, number of controls/labels = 30 pairs, duration = 4 minutes. We used 17 transverse slices with 7 mm thickness, FOV of 240 × 240 mm^2, and in-plane resolution of 3 × 3 mm^2.

Cerebravascular reactivity (CVR) was assessed by the measurement of blood oxygenation level-dependent (BOLD) MRI signal before and during inhalation of 5% CO_2 (mixed with 21% O_2 and 74% N_2). The measurement followed protocols established in Yezhuvath et al (31). Briefly, hypercapnia was administered via a Douglas bag (Harvard Apparatus, Holliston, MA) connected to a two-way valve. A research assistant was inside the magnet room throughout the experiment to switch the valve and to monitor the subject. Physiological parameters, including end-tidal (Et) CO_2, breathing rate, heart rate, and arterial oxygenation (sO_2), were monitored and recorded during the experiment (MEDRAD, Pittsburgh, PA; and Novametrix Medical Systems, Wallingford, CT). BOLD MR imaging used a single-shot gradient echo planar imaging (EPI) sequence with TR/TE/flip angle = 3000 msec/30 msec/90°, FOV = 220 × 220 mm^2, in-plane resolution = 2.8 × 2.8 mm^2, 25 transverse slices with 6 mm thickness, 141 volumes, and duration = 7 minutes.

BBB leakage was assessed by a contrast-enhanced vascular-space-occupancy (VASO) technique (27,32), which is based on the difference between pre- and postcontrast VASO signal intensities. The scan protocol included a precontrast scan, an injection of a contrast agent by an MRI-compatible power injector (MEDRAD, Pittsburgh, PA), and a postcontrast scan. An FDA-approved contrast agent, Gd-DTPA (Magnevist), was used with a standard dosage (0.1 mmol/kg). The postcontrast VASO scan was initiated 2 minutes after the injection to allow the contrast agent to reach a steady state in the blood vessels. This technique has been previously used to study BBB leakage in different grades of glioma (33). The VASO imaging used a segmented spin echo EPI sequence with EPI factor = 7. Other imaging parameters were: FOV = 192 × 192 mm^2, in-plane resolution = 1.5 × 1.5 mm^2, *k*-space matrix size = 128 × 128, 32 coronal slices with 5 mm thickness, fold-over direction = right–left, inversion time = 1088 msec (34), TR/TE/flip angle = 6000 msec/3.4 msec/90, and duration = 2.5 minutes.

In addition, two structural MRI scans were performed. A DTI scan was performed using a single-shot spin echo EPI, 30 diffusion-encoding directions (35) with b-factor of 1000 s/mm^2, TR/TE/flip angle = 5281msec/51msec/90°, 60 transverse slices, slice thickness = 2 mm (gap = 1 mm), FOV = 224 × 224 mm^2, and in-plane resolution = 2 × 2 mm^2. A T1-weighted high-resolution (1 × 1 × 1 mm^3) image was acquired using a standard magnetization-prepared rapid acquisition of gradient echo (MPRAGE) sequence (36).

Data Analysis

Images from the vascular scans were spatially coregistered to the FLAIR images using Statistical Parametric Mapping (SPM, University College London, UK) software. Leukoaraiosis regions were identified from FLAIR images (Fig. 1e) using a semiautomatic method described previously (37). Briefly, the FLAIR images were skull-stripped and the

voxels with signal intensity greater than 2 standard deviations above average were delineated as possible lesions. This was followed by manual editing to remove spurious voxels due to fat signal, motion effect, edge effect, or coil sensitivity inhomogeneity.

For comparison, regions of interest (ROIs) for NAWM were also obtained for each subject. Care was taken to avoid partial voluming with gray matter or lesion tissues. The identification of NAWM was conducted in three steps. In the first step, SPM was used to perform brain segmentation on the MPRAGE images (Fig. 1a), which yielded a white matter probabilistic map (Fig. 1b). The voxels with white matter probability greater than 90% were labeled (Fig. 1c). In the second step, the white matter lesion (Fig. 1d) voxels were removed from the white matter mask, resulting in a preliminary NAWM ROI (Fig. 1f). In the third step, potential partial-volumed voxels (for both gray-white partial voluming and normal-lesion partial voluming) were removed by iteratively shrinking the preliminary ROI by five times (Fig. 1g–k). Given that our voxel size was 0.45 mm, five iterations were chosen in order to shrink the ROI by 2.3 mm in every direction, which is comparable to the thickness of gray matter. We can therefore ensure that no gray matter was included in our final NAWM ROI (Fig. 1k).

Data processing for the three vascular imaging scans followed procedures previously established. CBF images were calculated from the difference between control and label images obtained from PCASL MRI (38,39). CVR maps in units of %BOLD/mmHg $EtCO_2$ were computed based on a linear regression between the $EtCO_2$ trace and the BOLD signal time-course (31). For BBB leakage, the VASO signal difference between pre- and postcontrast images, denoted by ΔVASO, was obtained and written as percentage of equilibrium magnetization (27). As shown in previous studies (33), ΔVASO reflects a combined effect of cerebral blood volume (CBV) and BBB leakage. To separate these two components, the CBV effect was estimated from the group-averaged CBF data using the well-known CBV/CBF relationship (40), $CBV = CBF^{\alpha}$. Thus, the BBB leakage, K_{BBB}, can be calculated by:

$$K_{BBB}=\Delta\mathrm{VASO}_L - \Delta\mathrm{VASO}_N \cdot \left(\frac{\mathrm{CBF}_L}{\mathrm{CBF}_N}\right)^{\alpha} \quad [1]$$

where the subscripts *L* and *N* denote values in leukoaraiosis and NAWM, respectively. The value of α was chosen to be 0.38 based on the literature (40), but a range of other values were also tested. Note that the leakage in NAWM was assumed to be 0 in this calculation.

We used DTI studio (Johns Hopkins University, Baltimore, MD) for the analysis of DTI images. Images with diffusion weighting were registered to the image acquired without diffusion gradients to correct for distortions due to eddy currents. The diffusion tensor was then calculated for each voxel, from which mean diffusivity (MD) and fractional anisotropy (FA) were calculated.

The subjects in this study were divided into two groups based on whether the ratio between leukoaraiosis volume and intracranial volume is greater or smaller than 0.1%. Those with a value greater than 0.1% were referred to as “subjects with significant leukoaraiosis”; those with a value smaller than 0.1% were referred to as “subjects without significant leukoaraiosis.” For the former group, vascular parameters in leukoaraiosis regions were compared to those in the NAWM regions. For the latter group, vascular parameters in the high-risk regions were measured to assess the potential vascular deficit in the absence of FLAIR hyperintensity.

Results

The volume of leukoaraiosis varied considerably among the elderly subjects studied (ranging from 0.012% to 1.194% of the intracranial volume). Ten subjects in the CBF/CVR study and 13 subjects in the BBB leakage study met our criterion for subjects with significant leukoaraiosis. Figure 2 shows the averaged parametric maps of CBF, CVR, ΔVASO, MD, and FA as well as the occurrence map of leukoaraiosis. Table 1 summarizes the comparison between parameters in leukoaraiosis and NAWM regions. A significant deficit was found for all three vascular parameters assessed.

In subjects without significant leukoaraiosis the CBF value in regions with a high risk for leukoaraiosis (the colored voxels in Fig. 2f) was found to be 23.6 ± 4.0 ml/min/100 ml (N = 7, mean ± SEM), which was significantly lower ($P < 0.001$) than that in the other white matter regions for the same subjects (32.1 ± 4.6). This finding suggests that these white matter regions have intrinsically lower CBF, which may explain why these regions have a higher probability to develop leukoaraiosis. It should be noted, however, that the extent of reduction (28.2 ± 2.2%) was milder when compared to the fully developed leukoaraiosis (Table 1). A similar finding was obtained from the CVR data. The high-risk regions had a lower CVR as compared to that in other white matter regions ($P = 0.07$).

These vascular changes were accompanied by structural damage, which was measured with MD and FA (Table 1). Furthermore, a significant correlation ($r = 0.64$, $P = 0.019$) was found between MD and K_{BBB} (Fig. 3), suggesting a possible link between vascular damage and tissue structural integrity.

NAWM in subjects with significant leukoaraiosis also showed signs of vascular damage. The CVR value in NAWM (0.066 ± 0.004 %BOLD/mmHg) was lower than that of equivalent regions in subjects without significant leukoaraiosis (0.082 ± 0.009 %BOLD/mmHg). Furthermore, among the subjects with significant leukoaraiosis, CVR in NAWM was correlated with leukoaraiosis volume ($r = 0.63$, $P = 0.05$) (Fig. 4). No correlations were found between leukoaraiosis volume and CBF, $\Delta VASO_N$, MD, or FA in NAWM ($P > 0.21$).

Discussion

In this study we show in vivo evidence of a vascular dysfunction in leukoaraiosis. Such changes appear to include multiple domains of vascular properties. Both CBF, a parameter reflecting the blood supply to the tissue, and CVR, an index related to the vascular reserve, are reduced in leukoaraiosis regions, providing strong evidence that the condition is associated with vascular alterations. Apart from the ischemic component, the vascular damage also seems to involve the integrity of the BBB. A compromised BBB may allow the extravasation of serum protein and cause toxicity to tissue. Interestingly, both BBB integrity and vascular reserve are associated with endothelium function, suggesting a central role of vascular endothelium in the formation of leukoaraiosis, which is consistent with the recent hypothesis of O'Sullivan and colleagues (1,41).

Our results confirmed findings from previous studies that report that CBF in leukoaraiosis is lower than that in NAWM (42–45). Furthermore, we showed that, even without leukoaraiosis, CBF in these high-risk regions is already lower than other white matter regions. Such a change was observed in the elderly subjects without significant leukoaraiosis, and was also confirmed in young healthy subjects (data not shown). This finding suggests that these white matter regions (often in deep brain tissue close to lateral ventricles; see Fig. 2f) have intrinsically low CBF, perhaps because they are located at the end of the vascular tree. Consequently, they are most susceptible to vascular deficits and the damage becomes more apparent with aging.

CBF in the gray matter is known to be coupled to energy demand and metabolism (46), which forms the basis of several brain mapping techniques such as functional MRI, positron emission tomography (PET), and optical imaging. Assuming that the coupling of blood flow and metabolic rate is also valid in the white matter, the observation of a reduced CBF in leukoaraiosis would not necessarily suggest vascular damage, since diminished metabolic demand in white matter (from axons and glial cells) may also cause a decrease in CBF (47). Therefore, in this study we further showed a CVR deficit in leukoaraiosis regions using hypercapnia as a vascular-specific challenge. The CVR deficit is particularly relevant in view of previous pathological findings of a thickening vascular wall (22,23) and may be a more specific marker for leukoaraiosis (43,48,49). We also found that CVR in NAWM of the subjects with significant leukoaraiosis is already lower than that in white matter of subjects without significant leukoaraiosis and that there is a correlation between NAWM CVR and size of leukoaraiosis. These suggest that CVR appears to be an early event in the cascade of pathogenesis and may precede the manifestation of lesion.

Our observation of a reduced CBF and CVR in the regions that have a high risk for leukoaraiosis is in agreement with recent studies reporting that white matter areas with lower perfusion correspond to locations of higher occurrence frequency of leukoaraiosis (42,50). A study in young healthy subjects (49) also reported that CVR is small or even negative in the high-risk regions. The findings that both CBF and CVR are compromised in the high-risk regions support the hypothesis that the pathogenesis of leukoaraiosis may be associated with ischemic conditions due to the episodic reduction of systemic arterial blood pressure (49,51).

In this study, we also provided experimental evidence that vascular deficits may cause white matter lesions via mechanisms other than ischemia. Specifically, we showed that BBB leakage is also present in leukoaraiosis regions, which may result in a direct insult to the parenchyma tissue. We used the relationship between CBF and CBV, known as Grubb's equation (40), to estimate the BBB leakage from ΔVASO. The coefficient α was assumed to be 0.38, based on the existing literature (40). However, we tested other α values ranging from 0.2 to 0.6, and found that the estimated BBB leakage was still significant. BBB leakage in leukoaraiosis has been previously studied using MR contrast agent methods where it was demonstrated that subjects with more severe leukoaraiosis tend to show higher BBB leakage (52,53). However, a direct comparison between leukoaraiosis and NAWM within the same subject has not been reported previously.

The structural changes in leukoaraiosis assessed by MD and FA are consistent with the previous findings (54). It has been suggested that tissue structural alteration assessed by DTI is linked to vascular dysfunction such as small vessel disease (55). Our data support this notion by showing that the BBB leakage is correlated with an increased MD.

The results of the present study should be interpreted in view of a few limitations. First, due to the complex procedures (eg, CO_2 inhalation, IV preparation, contrast agent administration) and long duration of the scans, the MRI measures mentioned above were not acquired from the same subjects. Instead, CBF and CVR were studied in one group of subjects ($n = 17$), and BBB leakage and diffusion were studied in another group ($n = 16$). We note, however, that there is no age difference between the groups ($P = 0.25$). Second, the CBF measurement used ASL MRI and this technique is known to be sensitive to arterial transit time of the blood (56). Thus, it is possible that part of the CBF difference between leukoaraiosis and NAWM is due to the differences in blood transit time. Additionally, the sample size in the present study is moderate and the *P*-values reported were not corrected for multiple comparisons. A further study with a larger number of subjects would be useful to confirm these findings.

In conclusion, leukoaraiosis regions are characterized by various forms of vascular damages including reduced blood supply, vascular reserve, and significant leakage in BBB. In addition, there are early signs of vascular damage even in NAWM and CVR appears to be a sensitive marker to detect such changes.

Acknowledgments

The authors are grateful to Dr. Matthias van Osch for providing the ASL pulse sequence and Sina Aslan for assistance with the data processing. We also thank Dr. Nyaz Didehbani for proofreading.

Contract grant sponsor: Alzheimer Association; Contract grant number: NIRG 05-14056; Contract grant sponsor: National Institutes of Health (NIH); Contract grant numbers: NIH R01 MH084021, NIH R21 NS054916, NIH P30 AG12300; Contract grant sponsors: American Heart Association, Texas Instruments Foundation.

References

1. O'Sullivan M. Leukoaraiosis. Pract Neurol. 2008; 8:26–38. [PubMed: 18230707]
2. Essig M, Hawighorst H, Schoenberg SO, et al. Fast fluid-attenuated inversion-recovery (FLAIR) MRI in the assessment of intraaxial brain tumors. J Magn Reson Imaging. 1998; 8:789–798. [PubMed: 9702879]
3. Liu CK, Miller BL, Cummings JL, et al. A quantitative MRI study of vascular dementia. Neurology. 1992; 42:138–143. [PubMed: 1734295]
4. Gootjes L, Teipel SJ, Zebuhr Y, et al. Regional distribution of white matter hyperintensities in vascular dementia, Alzheimer's disease and healthy aging. Dement Geriatr Cogn Disord. 2004; 18:180–188. [PubMed: 15211074]
5. Basile AM, Pantoni L, Pracucci G, et al. Age, hypertension, and lacunar stroke are the major determinants of the severity of age-related white matter changes. The LADIS (Leukoaraiosis and Disability in the Elderly) Study. Cerebrovasc Dis. 2006; 21:315–322. [PubMed: 16490940]
6. Dufouil C, de Kersaint-Gilly A, Besancon V, et al. Longitudinal study of blood pressure and white matter hyperintensities: the EVA MRI Cohort. Neurology. 2001; 56:921–926. [PubMed: 11294930]
7. Liao D, Cooper L, Cai J, et al. Presence and severity of cerebral white matter lesions and hypertension, its treatment, and its control. The ARIC Study. Atherosclerosis Risk in Communitues Study. Stroke. 1996; 27:2262–2270. [PubMed: 8969791]
8. Hainsworth AH, Markus HS. Do in vivo experimental models reflect human cerebral small vessel disease? A systematic review. J Cereb Blood Flow Metab. 2008; 28:1877–1891. [PubMed: 18698331]
9. Schmidt R, Scheltens P, Erkinjuntti T, et al. White matter lesion progression: a surrogate endpoint for trials in cerebral small-vessel disease. Neurology. 2004; 63:139–144. [PubMed: 15249623]
10. Wiszniewska M, Devuyst G, Bogousslavsky J, Ghika J, van Melle G. What is the significance of leukoaraiosis in patients with acute ischemic stroke? Arch Neurol. 2000; 57:967–973. [PubMed: 10891978]
11. Bots ML, van Swieten JC, Breteler MM, et al. Cerebral white matter lesions and atherosclerosis in the Rotterdam Study. Lancet. 1993; 341:1232–1237. [PubMed: 8098390]
12. Smith EE, Gurol ME, Eng JA, et al. White matter lesions, cognition, and recurrent hemorrhage in lobar intracerebral hemorrhage. Neurology. 2004; 63:1606–1612. [PubMed: 15534243]
13. Guttmann CR, Jolesz FA, Kikinis R, et al. White matter changes with normal aging. Neurology. 1998; 50:972–978. [PubMed: 9566381]
14. Schmidt R, Schmidt H, Kapeller P, et al. The natural course of MRI white matter hyperintensities. J Neurol Sci. 2002:203–204. 253–257.
15. Kraut MA, Beason-Held LL, Elkins WD, Resnick SM. The impact of magnetic resonance imaging-detected white matter hyperintensities on longitudinal changes in regional cerebral blood flow. J Cereb Blood Flow Metab. 2008; 28:190–197. [PubMed: 17534385]
16. Piguet O, Ridley L, Grayson DA, et al. Are MRI white matter lesions clinically significant in the ‘old-old’? Evidence from the Sydney Older Persons Study. Dement Geriatr Cogn Disord. 2003; 15:143–150. [PubMed: 12584429]

17. Soderlund H, Nyberg L, Adolfsson R, Nilsson LG, Launer LJ. High prevalence of white matter hyperintensities in normal aging: relation to blood pressure and cognition. Cortex. 2003; 39:1093–1105. [PubMed: 14584568]
18. Wen W, Sachdev P. The topography of white matter hyperintensities on brain MRI in healthy 60- to 64-year-old individuals. Neuroimage. 2004; 22:144–154. [PubMed: 15110004]
19. Yue NC, Arnold AM, Longstreth WT Jr, et al. Sulcal, ventricular, and white matter changes at MR imaging in the aging brain: data from the cardiovascular health study. Radiology. 1997; 202:33–39. [PubMed: 8988189]
20. Breteler MM, van Swieten JC, Bots ML, et al. Cerebral white matter lesions, vascular risk factors, and cognitive function in a population-based study: the Rotterdam Study. Neurology. 1994; 44:1246–1252. [PubMed: 8035924]
21. Gunning-Dixon FM, Raz N. The cognitive correlates of white matter abnormalities in normal aging: a quantitative review. Neuropsychology. 2000; 14:224–232. [PubMed: 10791862]
22. Lammie GA. Pathology of small vessel stroke. Br Med Bull. 2000; 56:296–306. [PubMed: 11092081]
23. Lammie GA, Brannan F, Slattery J, Warlow C. Nonhypertensive cerebral small-vessel disease. An autopsy study. Stroke. 1997; 28:2222–2229. [PubMed: 9368569]
24. Akiguchi I, Tomimoto H, Suenaga T, Wakita H, Budka H. Blood-brain barrier dysfunction in Binswanger's disease; an immuno-histochemical study. Acta Neuropathol. 1998; 95:78–84. [PubMed: 9452825]
25. Wallin A, Sjogren M, Edman A, Blennow K, Regland B. Symptoms, vascular risk factors and blood-brain barrier function in relation to CT white-matter changes in dementia. Eur Neurol. 2000; 44:229–235. [PubMed: 11096223]
26. Wardlaw JM, Sandercock PA, Dennis MS, Starr J. Is breakdown of the blood-brain barrier responsible for lacunar stroke, leukoaraiosis, and dementia? Stroke. 2003; 34:806–812. [PubMed: 12624314]
27. Lu H, Law M, Johnson G, Ge Y, van Zijl PC, Helpern JA. Novel approach to the measurement of absolute cerebral blood volume using vascular-space-occupancy magnetic resonance imaging. Magn Reson Med. 2005; 54:1403–1411. [PubMed: 16254955]
28. Dai W, Garcia D, de Bazelaire C, Alsop DC. Continuous flow-driven inversion for arterial spin labeling using pulsed radio frequency and gradient fields. Magn Reson Med. 2008; 60:1488–1497. [PubMed: 19025913]
29. Wong EC. Vessel-encoded arterial spin-labeling using pseudocontinuous tagging. Magn Reson Med. 2007; 58:1086–1091. [PubMed: 17969084]
30. Wu WC, Fernandez-Seara M, Detre JA, Wehrli FW, Wang J. A theoretical and experimental investigation of the tagging efficiency of pseudocontinuous arterial spin labeling. Magn Reson Med. 2007; 58:1020–1027. [PubMed: 17969096]
31. Yezhuvath US, Lewis-Amezcua K, Varghese R, Xiao G, Lu H. On the assessment of cerebrovascular reactivity using hypercapnia BOLD MRI. NMR Biomed. 2009; 22:779–786. [PubMed: 19388006]
32. Lu H, Golay X, Pekar JJ, Van Zijl PC. Functional magnetic resonance imaging based on changes in vascular space occupancy. Magn Reson Med. 2003; 50:263–274. [PubMed: 12876702]
33. Lu H, Pollack E, Young R, et al. Predicting grade of cerebral glioma using vascular-space occupancy MR imaging. AJNR Am J Neuroradiol. 2008; 29:373–378. [PubMed: 17974612]
34. Lu H, Clingman C, Golay X, van Zijl PC. Determining the longitudinal relaxation time (T1) of blood at 3.0 Tesla. Magn Reson Med. 2004; 52:679–682. [PubMed: 15334591]
35. Jones DK, Horsfield MA, Simmons A. Optimal strategies for measuring diffusion in anisotropic systems by magnetic resonance imaging. Magn Reson Med. 1999; 42:515–525. [PubMed: 10467296]
36. Brant-Zawadzki M, Gillan GD, Nitz WR. MP RAGE: a three-dimensional, T1-weighted, gradient-echo sequence—initial experience in the brain. Radiology. 1992; 182:769–775. [PubMed: 1535892]

37. Marquez de la Plata C, Ardelean A, Koovakkattu D, et al. Magnetic resonance imaging of diffuse axonal injury: quantitative assessment of white matter lesion volume. J Neurotrauma. 2007; 24:591–598. [PubMed: 17439343]
38. Aslan S, Xu F, Wang PL, et al. Estimation of labeling efficiency in pseudocontinuous arterial spin labeling. Magn Reson Med. 2010; 63:765–771. [PubMed: 20187183]
39. van Osch MJ, Teeuwisse WM, van Walderveen MA, Hendrikse J, Kies DA, van Buchem MA. Can arterial spin labeling detect white matter perfusion signal? Magn Reson Med. 2009; 62:165–173. [PubMed: 19365865]
40. Grubb RL Jr, Raichle ME, Eichling JO, Ter-Pogossian MM. The effects of changes in PaCO2 on cerebral blood volume, blood flow, and vascular mean transit time. Stroke. 1974; 5:630–639. [PubMed: 4472361]
41. Hassan A, Hunt BJ, O'Sullivan M, et al. Markers of endothelial dysfunction in lacunar infarction and ischaemic leukoaraiosis. Brain. 2003; 126(Pt 2):424–432. [PubMed: 12538408]
42. Brickman AM, Zahra A, Muraskin J, et al. Reduction in cerebral blood flow in areas appearing as white matter hyperintensities on magnetic resonance imaging. Psychiatry Res. 2009; 172:117–120. [PubMed: 19324534]
43. Marstrand JR, Garde E, Rostrup E, et al. Cerebral perfusion and cerebrovascular reactivity are reduced in white matter hyperintensities. Stroke. 2002; 33:972–976. [PubMed: 11935046]
44. O'Sullivan M, Lythgoe DJ, Pereira AC, et al. Patterns of cerebral blood flow reduction in patients with ischemic leukoaraiosis. Neurology. 2002; 59:321–326. [PubMed: 12177363]
45. Sakoglu U, Huisa-Garate B, Rosenberg GA, Sood R. Application of FT-based MMSE deconvolution method for cerebral blood flow measurement in patients with leukoaraiosis. Magn Reson Imaging. 2009; 27:625–630. [PubMed: 19121907]
46. Roy CS, Sherrington CS. On the regulation of the blood-supply of the brain. J Physiol. 1890; 11:85–158. 17.
47. Villringer A, Dirnagl U. Coupling of brain activity and cerebral blood flow: basis of functional neuroimaging. Cerebrovasc Brain Metab Rev. 1995; 7:240–276. [PubMed: 8519605]
48. Bakker SL, de Leeuw FE, de Groot JC, Hofman A, Koudstaal PJ, Breteler MM. Cerebral vasomotor reactivity and cerebral white matter lesions in the elderly. Neurology. 1999; 52:578–583. [PubMed: 10025791]
49. Mandell DM, Han JS, Poublanc J, et al. Selective reduction of blood flow to white matter during hypercapnia corresponds with leukoaraiosis. Stroke. 2008; 39:1993–1998. [PubMed: 18451357]
50. Holland CM, Smith EE, Csapo I, et al. Spatial distribution of white-matter hyperintensities in Alzheimer disease, cerebral amyloid angiopathy, and healthy aging. Stroke. 2008; 39:1127–1133. [PubMed: 18292383]
51. Pantoni L, Garcia JH. Pathogenesis of leukoaraiosis: a review. Stroke. 1997; 28:652–659. [PubMed: 9056627]
52. Topakian R, Barrick TR, Howe FA, Markus HS. Blood-brain barrier permeability is increased in normal-appearing white matter in patients with lacunar stroke and leucoaraiosis. J Neurol Neurosurg Psychiatry. 2010; 81:192–197. [PubMed: 19710048]
53. Wardlaw JM, Farrall A, Armitage PA, et al. Changes in background blood-brain barrier integrity between lacunar and cortical ischemic stroke subtypes. Stroke. 2008; 39:1327–1332. [PubMed: 18309161]
54. Bastin ME, Clayden JD, Pattie A, Gerrish IF, Wardlaw JM, Deary IJ. Diffusion tensor and magnetization transfer MRI measurements of periventricular white matter hyperintensities in old age. Neurobiol Aging. 2009; 30:125–136. [PubMed: 17624630]
55. Nitkunan A, Barrick TR, Charlton RA, Clark CA, Markus HS. Multimodal MRI in cerebral small vessel disease: its relationship with cognition and sensitivity to change over time. Stroke. 2008; 39:1999–2005. [PubMed: 18436880]
56. Bastos-Leite AJ, Kuijer JP, Rombouts SA, et al. Cerebral blood flow by using pulsed arterial spin-labeling in elderly subjects with white matter hyperintensities. AJNR Am J Neuroradiol. 2008; 29:1296–1301. [PubMed: 18451090]

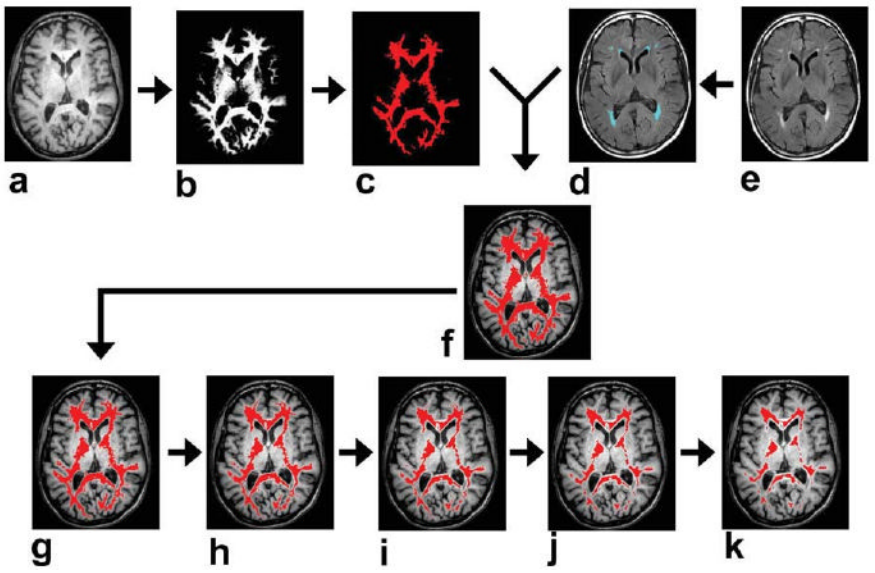

Figure 1.

Procedures for identification of NAWM ROI. **a:** T1 weighted image. **b:** White matter probability map obtained from the segmentation of T1-weighted image. Black and white voxels indicate 0 and 100% probability, respectively. **c:** Voxels with white matter probability greater than 90%. **d:** White matter lesions (blue voxels) overlaid on FLAIR image. **e:** FLAIR image. **f:** A preliminary NAWM ROI (red voxels) overlaid on FLAIR image. **g–k:** The preliminary NAWM ROI was shrunken iteratively for five times with each time removing one layer of voxels at the edge. This step is useful in minimizing partial voluming effect.

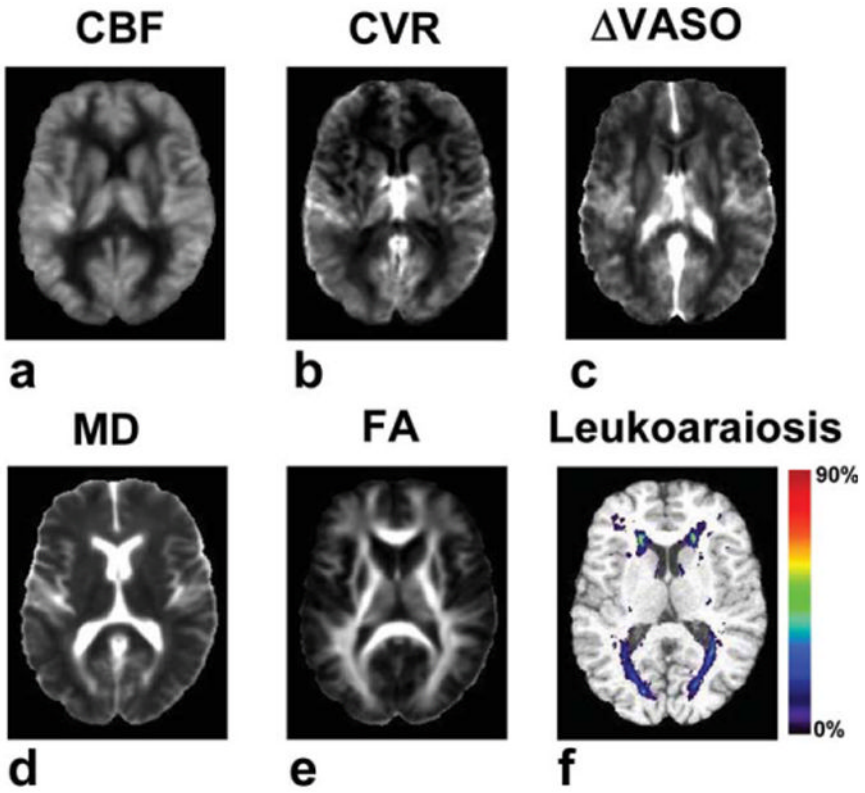

Figure 2.

Averaged parametric maps of CBF, CVR, ΔVASO, MD, and FA. All images were spatially registered to a brain template and then averaged. For the ΔVASO images, part of the occipital and frontal pole was missing in a few subjects due to incomplete brain coverage. For these regions the ΔVASO map was based on the data available for the location. An occurrence map of leukoaraiosis is also shown. For each voxel the probabilistic value was calculated by dividing the number of subjects having leukoaraiosis at the location by the total number of subjects (n = 33). [Color figure can be viewed in the online issue, which is available at http://www.interscience.wiley.com.]

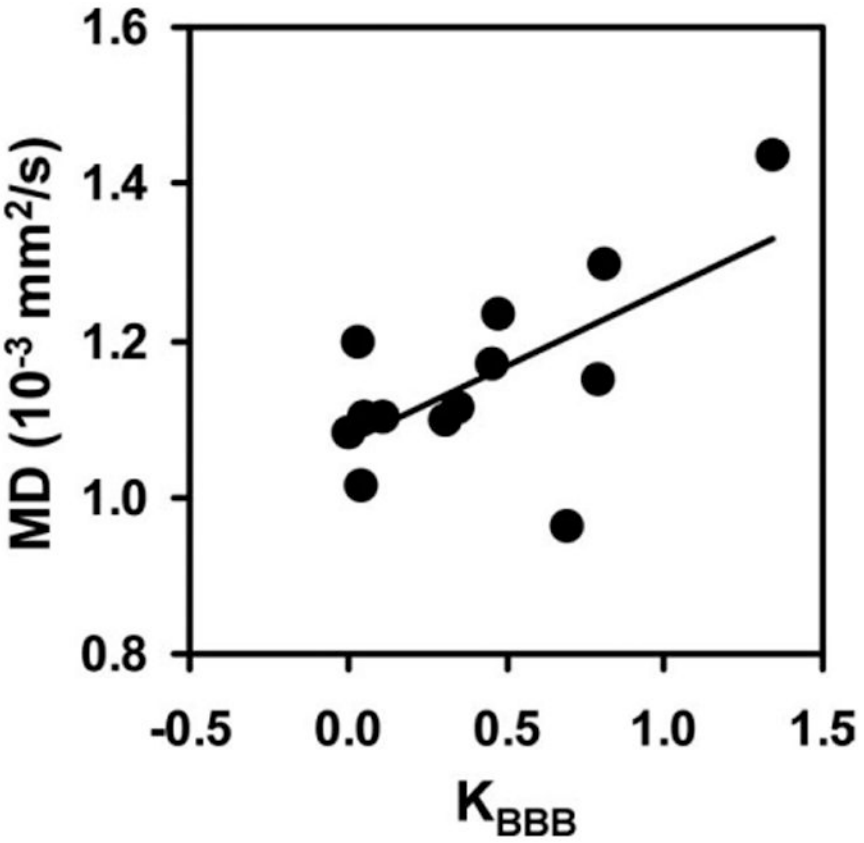

Figure 3.
Correlation between MD and K_{BBB} across individuals ($r = 0.64$, $P = 0.019$; $n = 13$). K_{BBB} was calculated using Eq. [1]. MD was obtained from DTI data.

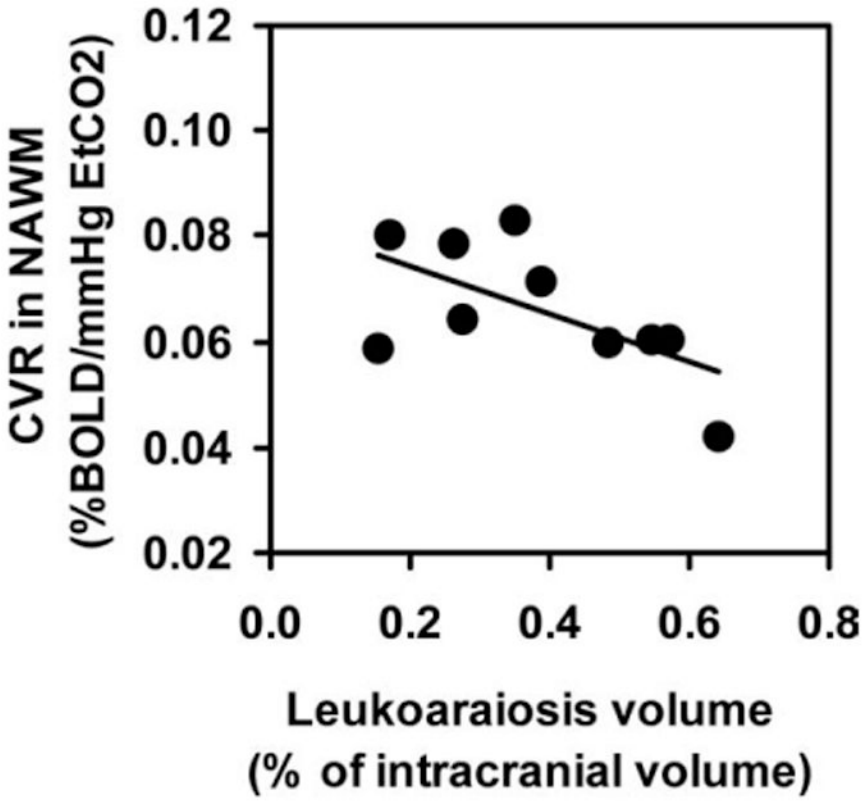

Figure 4.
Correlation between CVR in NAWM and the leukoaraiosis volume ($r = 0.63$, $P = 0.05$; $n = 10$). The leukoaraiosis volume is presented in the percentage of the intracranial volume to account for brain size differences.

Table 1

Comparison of Physiological Parameters Between NAWM and Leukoaraiosis

Parameter	NAWM (mean ± SEM)	Leukoaraiosis (mean ± SEM)	% change (mean ± SEM)	*P*-value	*N*
CBF (ml/min/100 ml brain)	33.5 ± 1.9	13.4 ± 2.0	-60.3 ± 5.2	< 0.001	10
CVR (%BOLD/mmHg)	0.066 ± 0.004	0.035 ± 0.009	-47.5 ± 11.6	0.005	10
K_{BBB} (%)	0*	0.42 ± 0.11	N/A	0.003	13
MD($10^{-3}mm^2/s$)	0.783 ± 0.008	1.151 ± 0.034	47.0 ± 3.9	< 0.001	13
FA	0.400 ± 0.005	0.240 ± 0.009	-39.9 ± 2.2	< 0.001	13

*In the calculation of K_{BBB} it was assumed that the leakage in NAWM is 0. Thus, this value in the table is 0 for all subjects.